EPR in the 21st Century
A Kawamori, J Yamauchi and H Ohta (Editors)

Modern ESR methods in studies of the dynamic structure of proteins and membranes

Jack H. Freed
Baker Laboratory of Chemistry and Chemical Biology, Cornell University and
National Biomedical Center for Advanced ESR Technology (ACERT)

A review of modern electron spin resonance (ESR) techniques for studying the dynamic structure of proteins and membranes using nitroxide spin labels is presented. In particular multiple quantum coherence FT-ESR, multifrequency ESR based on high frequency ESR and two dimensional ESR to study the structure and dynamics of bio-membranes and proteins are illustrated by several examples. Distances in biomolecules have been determined accurately. The details of complex dynamics in proteins and the dynamic structure of membranes were characterized.

1. INTRODUCTION

ESR spectroscopy, based on nitroxide spin labeling, is largely driven by the sensitivity of the nitroxide label to its surroundings. The interaction of the unpaired electron spin of nitroxide with the ^{14}N magnetic nucleus ($I = 1$) leads to an electron nuclear dipolar (or hyperfine (*hf*)) tensor, which for rapidly tumbling molecules averages to a nonzero value. This is also the case for the g tensor of the electron spin, which, when averaged, yields the isotropic g shift. If the investigated system (e.g., a membrane) is macroscopically aligned, then one can observe the different "single-crystal-like" spectra obtained for each orientation of the system with respect to the static magnetic field. The homogeneous line broadening (*hb*) of the spectra would then reflect the motional dynamics.

ESR spectra are known to change dramatically as the tumbling motion of the probe slows, thus providing great sensitivity to fluidity in the neighborhood of the probe [1]. An approach based on the stochastic Liouville equation, known as slow motion theory, has been developed [2], which shows that the dramatic line shape changes are particularly sensitive to the microscopic detail of the dynamics. These methods of analysis enable a quantitative assessment of ESR spectra in terms of motional rates of spinning of the nitroxide moiety, the end-over-end tumbling of the tagged molecule, and local environmental constraints on the motion.

For a spin-labeled protein, for example, the motions could be the spinning of the tether attaching the nitroxide and the overall tumbling of the protein. In a bilayer, typical of a cell membrane, reorientation of the lipids is constrained by the surrounding lipids and other molecules. The motional rates lead to a rotational diffusion tensor, whereas the motional constraints lead to an orientational order parameter.

The changes in magnitude of the *hf* splitting and g value can be used to monitor features of the local surroundings, such as its polarity. In addition, unpaired electron spins from different

nitroxides (on the same or different molecules) interact weakly through long-range magnetic dipolar interactions or strongly through short range Heisenberg spin exchange. In fluid media, these latter interactions can be used to monitor microscopic translational dynamics [3]. In frozen or very viscous media the dipolar interactions can be used to measure distances, either, by continuous wave (cw) ESR or pulsed ESR [4,5].

Often, one must deal with the complications of samples that are MOMD (i.e. microscopically ordered but macroscopically disordered)[2]. Membrane vesicles offer a physical example of this property. Spin-labeled moieties in the different vesicle regions may be oriented at all angles with respect to the magnetic field, thus providing a "powder-like" spectrum with inhomogeneous line broadening (*ib*) superimposed on the *hb*.
The degree of *ib* is determined by the extent of local (microscopic) ordering. This *ib* masks the *hb*, resulting in reduced resolution to dynamic and ordering parameters. Despite this, modeling of the heterogeneity and of the dynamic effects to fit the ESR spectrum can yield important insights.

2. DOUBLE QUANTUM COHERENCE AND DISTANCE MEASUREMENTS

The determination of intra- and inter-molecular distances has become an important application of contemporary ESR spectroscopy. Areas of interest include the structure of protein complexes and functional dynamics of proteins that are neither soluble nor crystallized

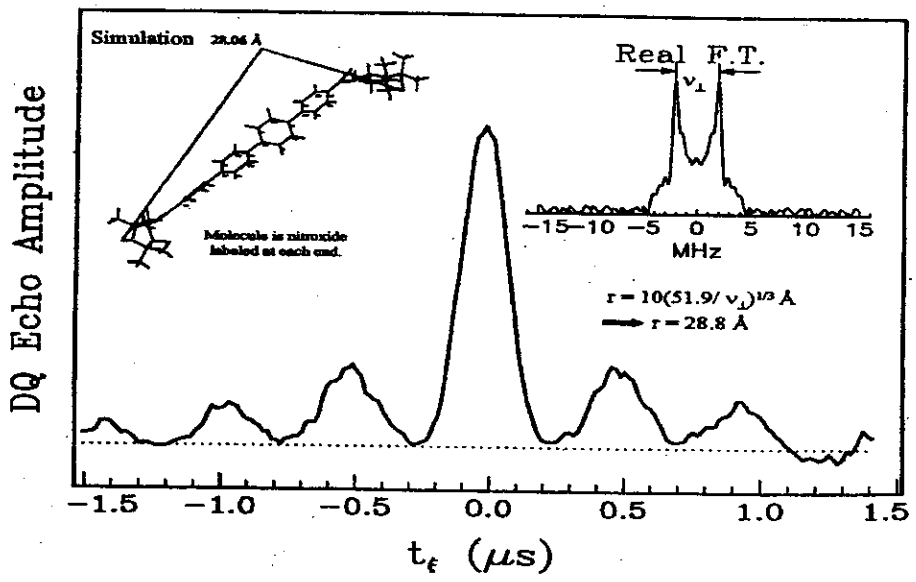

Figure 1. **(Left)** The doubly labeled molecule is dissolved in a frozen amorphous matrix. **(Bottom)** The maximum echo signal recorded as a function of $t_\xi = t_2 - t_p$ (See ref. [6a] for the 6 pulse DQC sequence applied). **(Right)** A Fourier transform of this echo signal yields the Pake-type dipolar spectrum in the frequency domain. The separation $\nu_\perp$ of the two sharp peaks is directly related to the distance r between the labels $r \propto \nu_\perp^{-1/3}$. The calculated value of the distance 28.8 Å is close to the value 28.06 Å obtained by a model simulation [6a].

[4].

Strong Double Quantum Coherence (DQC) signals for a variety of bilabeled nitroxide

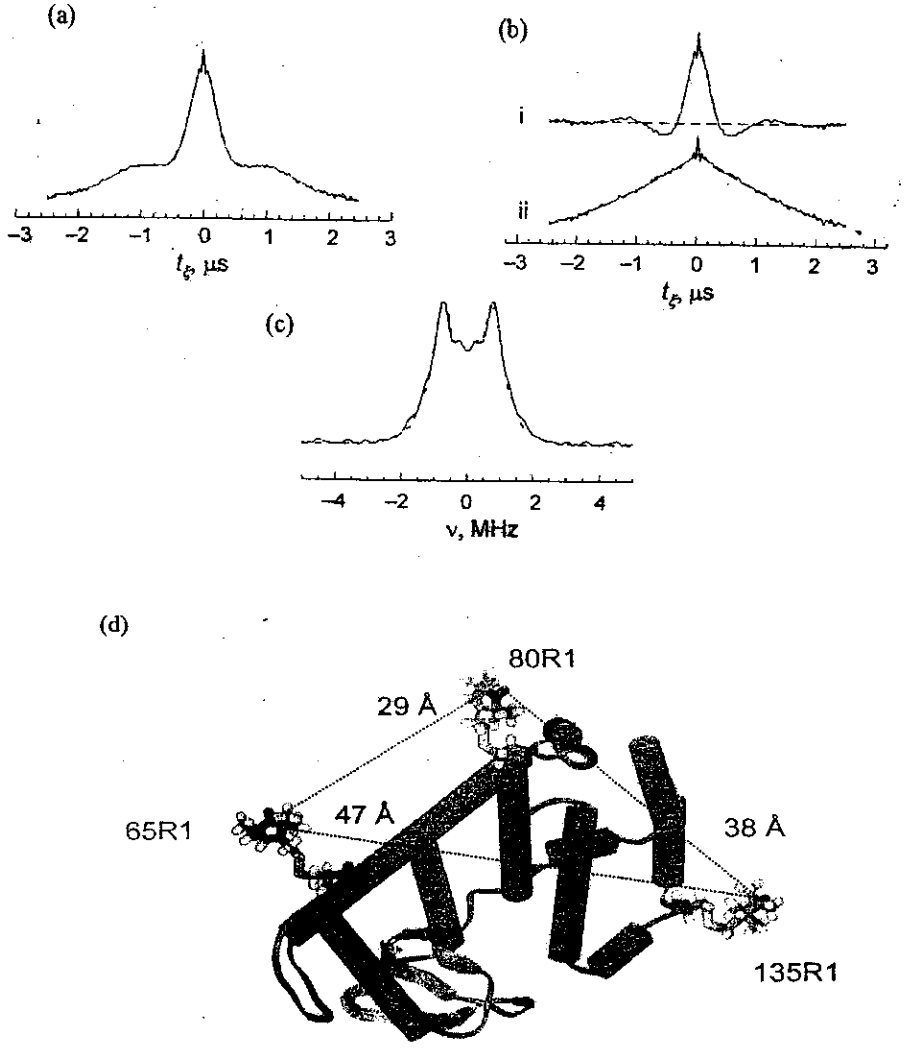

Figure 2. Long distances in T4 Lysozyme obtained from DQC experiment [6b]. (a) The DQC signal obtained for the double labeled mutant 65/86. (b) This signal can be separated into (i) the intramolecular signal and (ii) a baseline from the intermolecular signal. (c) Fourier transformed spectrum from (i). Broken lines show the simulations with R_{av} = 37.4 Å and ΔR = 2.7 Å. (d) Molecular modeling showing three distances in three double labeled DQ experiments.

molecules in both disordered and oriented solids have been achieved recently [6a,6b] as shown in Fig. 1. For a benchmark, (a distance of 28.8 ± 0.05 Å between the two nitroxide groups) the rigid linear biradical, piperidinyl-CO_2-(phenyl)-O_2C-piperidinyl, was obtained (versus 28.06 Å from molecular modeling).

Another example, T4-Lysozyme double labeled mutant 65/86 shows a distance of 37 Å between the unpaired electrons on each of the two labels. The echo signal and its Fourier transformed frequency spectrum are shown in Fig. 2 (a), (b) and (c). In this case, a baseline signal due to the intermolecular DQ signal subtracted before Fourier transformation. In simulation the distribution of the distance has been assumed. The distances obtained are consistent with the known crystal structure of T4-Lysozyme and the conformations of the nitroxide tether.

3. MULTIFREQUENCY ESR BASED ON HIGH FREQUENCY ESR

3.1. Virtues of High Frequency ESR

The snapshot feature of cw ESR encourages a multifrequency approach to the study of the complex modes of motion of proteins, DNA, and other polymers, enabling the decomposition of these modes according to their different time scales [7]. The degree and nature of the line broadening is a function of the frequency applied. For example, in the case of proteins, the higher frequency ESR should "freeze out" the slow overall tumbling motion, leaving only faster internal modes of motion. Alternatively, ESR performed at lower frequencies would

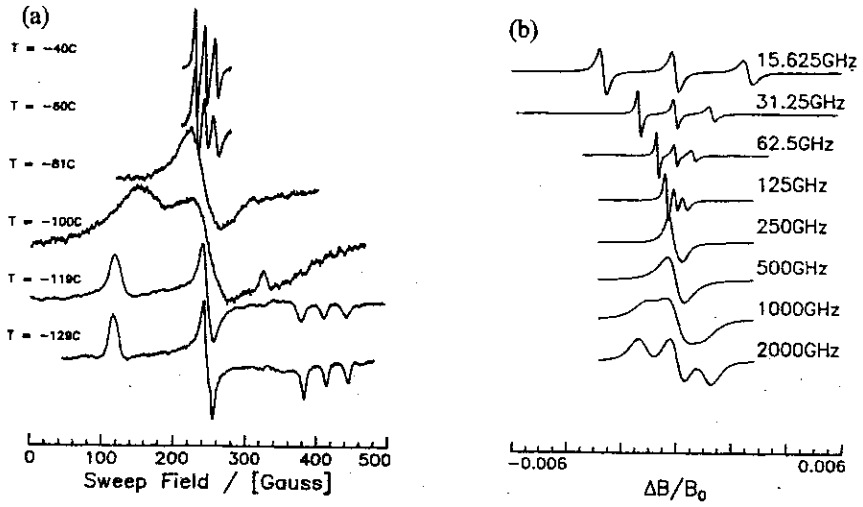

Figure 3. (a) Nitroxide cw ESR spectra observed at 250 GHz change dramatically with temperature caused by the slowing down of the tumbling motion with decreasing temperature. The uppermost two spectra, –40 and –60 °C, correspond to the motional narrowing regime, the middle –81 and –100 °C to the slow motional regime, and the lowest – 119 and –129 °C to the rigid limit. (b) The derivative ESR simulations for characteristic ESR frequencies demonstrate the snapshot property of ESR when spin-labeled molecules are tumbling with correlation time $\tau_R = 1.7 \times 10^{-9}$ sec. The spectra observed at 15.6 to 125 GHz in (b) correspond to the motional narrowing regime and the spectra observed at 500 and 1000 GHz to the slow motional regime [13].

be sensitive to the motions on a slower time scale.

Fig. 3 (a) shows changes of spectra with decreasing temperature observed for PDT/Toluene at 250 GHz. The spectra observed at –40 and –60 °C show three sharp *hf* lines corresponding to the motional narrowing regime. The spectra at – 81 and –100 °C show a gradual change to the slow motional regime. Those at – 119 and –129 °C correspond to the rigid limit.

Instead of changing temperature, a change in ESR frequency manifests almost the same phenomena as shown in Fig. 3 (b). A motional process that looks fast at lower frequencies will look slow at higher frequencies. This means that for complex dynamics of proteins the fast motions will show up best at higher frequencies, whereas the slower overall and collective motions will show up best at lower frequencies.

3.2. Protein and DNA Dynamics

Fig. 4 (a) illustrates the complex motions of spin labeled T4 Lysozyme in aqueous solution [7,8] which consist of spin label reorientation, side chain fluctuation and global tumbling. Fig. 4(b)[9] depicts the fluctuating side chain. In the MOMD model, the global tumbling rate tends to zero.

The virtues of such an approach were demonstrated in a study at 9 and 250 GHz on spin-labeled mutants of T4 lysozyme in aqueous solution [8]. On the short time scale of the 250-GHz ESR experiment, the overall tumbling was too slow to affect the spectrum; thus, a MOMD analysis provided a satisfactory modeling of the overall tumbling, and HF-enhanced spectral resolution reported on the internal dynamics (Fig. 5b). The analysis of the 9 GHz spectra was more complex, because the longer time scale did not freeze out the overall

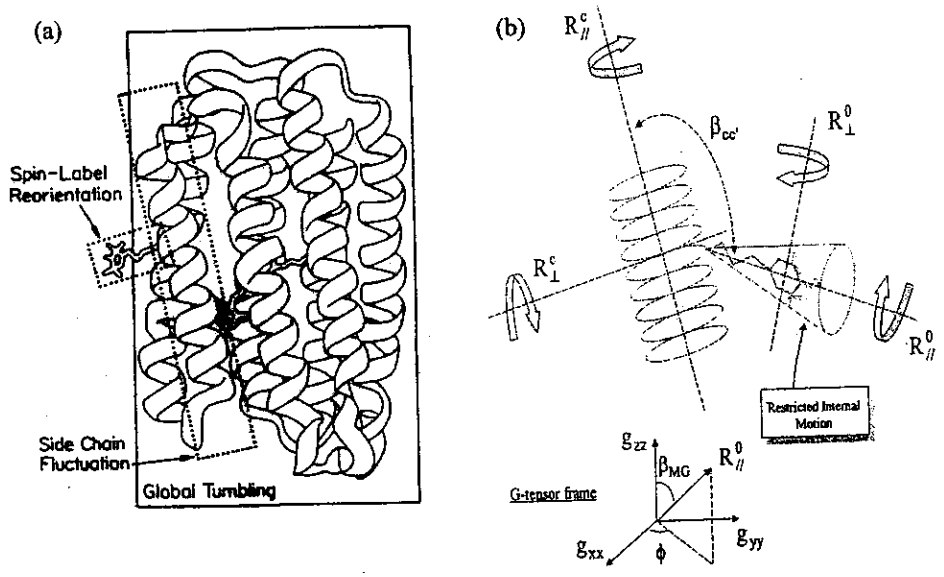

Figure 4. (a) Protein Dynamics of Spin-labeled T4-Lysozyme: There are three kind of motions, spin-label reorientation, side chain fluctuations and global tumbling. (b) The SRLS model is illustrated including relevant motional parameters [7,9].

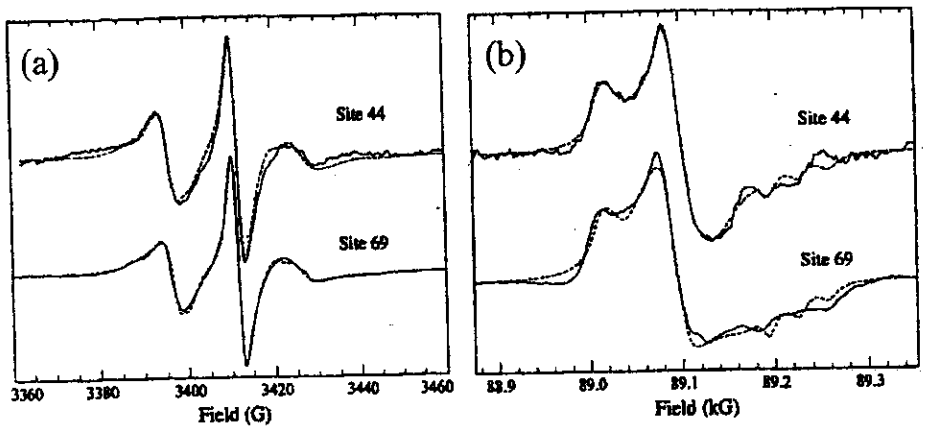

Figure 5. ESR spectra of spin labeled T4 Lysozyme. (a) 9 GHz spectra are affected by overall tumbling. (b) 250 GHz ESR spectra show nitroxide motion about the tether and of the peptide backbone [8]. The upper (lower) curves are for T4 lysozyme mutants labeled at site 44 (69).

tumbling motion. The slowly relaxing local structure (SRLS) model [7] simultaneously incorporated both the internal and overall motions. By fixing the internal motional parameters at the values obtained from 250 GHz data, fits to the 9-GHz line shapes generated by SRLS successfully yielded the rate for the global dynamics. This demonstrated how these different modes can be distinguished using the multi-frequency ESR approach. The analysis also indicated that $R^0_\perp$ reflects the backbone protein motion.

A related ESR study was performed on spin-labeled DNA oligomers [9]. The dynamic modes and spin label are illustrated in Fig. 6. The results show two conformers which are distinguished by their ordering. $R^0_\perp$ decreases with increasing oligomer length, strongly suggesting that backbone motion is being sensed. Note that for DNA oligomers, the overall

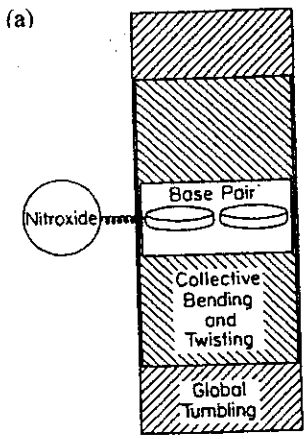

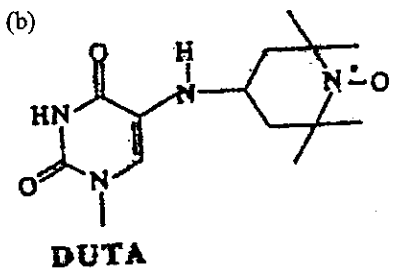

Figure 6. (a) Dynamics of spin-labeled DNA, (b) Molecular formula of spin label DUTA [9].

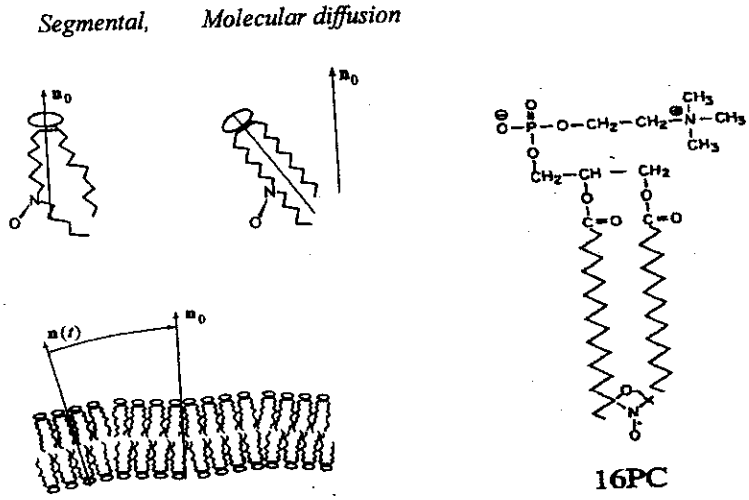

Figure 7. (a) The spin labeled PC experiences two kinds of motions: segmental diffusion and molecular diffusion. $\mathbf{n}_0$ shows the average direction of the membrane normal and $\mathbf{n}(t,)$ in the lower insert, shows the fluctuating normal due to slow director fluctuations. (b) shows the chemical structure of spin label 16PC, [11].

tumbling may be analyzed by use of hydrodynamic theory.

3.3 Dynamic Structure of Membranes

We have been studying model membrane vesicles consisting of di-palmitoy-lphosphatidyl-choline (DPPC) in excess water. The spin label is incorporated in the membrane and EPR spectra of the label are observed in various membrane systems over a range of temperatures. The dynamics of a labeled lipid in a membrane is illustrated in Fig.7.

Cholesterol is an important regulator of the physical properties of biological membranes and their functions. When added to model membranes of pure lipid in the liquid crystalline (LC) phase, it leads to a new phase, the liquid ordered (LO) phase, which is more ordered yet fluid. Spin label 16PC (cf. Fig. 7b) was observed by ESR at 250GHz vs. temperature for pure DPPC vesicles (Fig. 8 left) and for vesicles of DPPC and cholesterol in ratio 1:1 (Fig. 8 right), [11]. These spectra and equivalent ones obtained at 9GHz were fit by the MOMD model to yield rotational diffusion tensors components $R_\perp$ and $R_{||}$ and order parameters, S (cf. Fig. 9). Based on these recent results [11], the following conclusions can be derived:

(1) 250 vs. 9 GHz spectra reveal that simple MOMD analyses show typical discrepancies in their predictions of ordering and dynamics.

(2) SRLS fits to 9 GHz do however lead to consistency with the 250 GHz MOMD results for the internal dynamics and ordering. In addition they show that overall tumbling rate constants are $1-3\times10^{-7}s^{-1}$ and overall order parameters are approximately 0.5.

(3) The LO phase shows faster end-chain motions over the LC phase and some increased local ordering, with some increase in overall ordering, but little change in overall motional parameters.

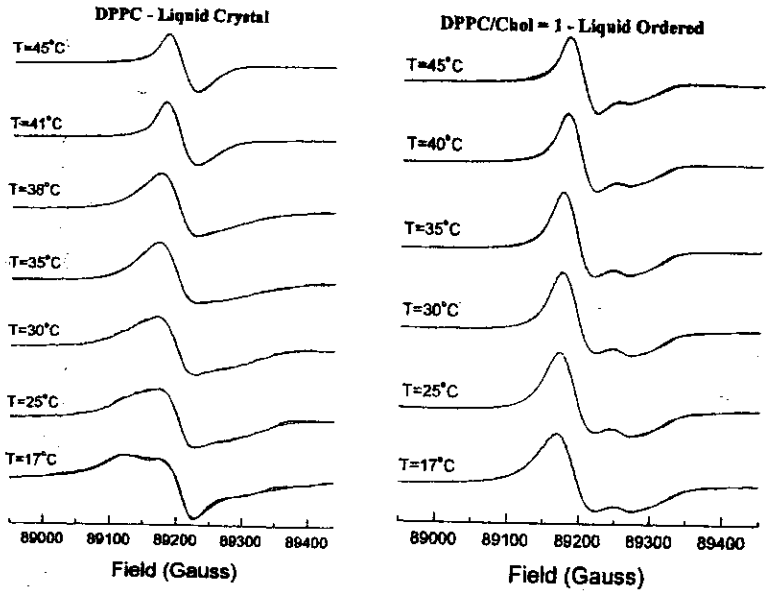

Figure 8. 250 GHz ESR Spectra of 16 PC in a liquid crystal and cholesterol membranes and their MOMD fits [11]. The experimental results and fitting curves are almost coincident.

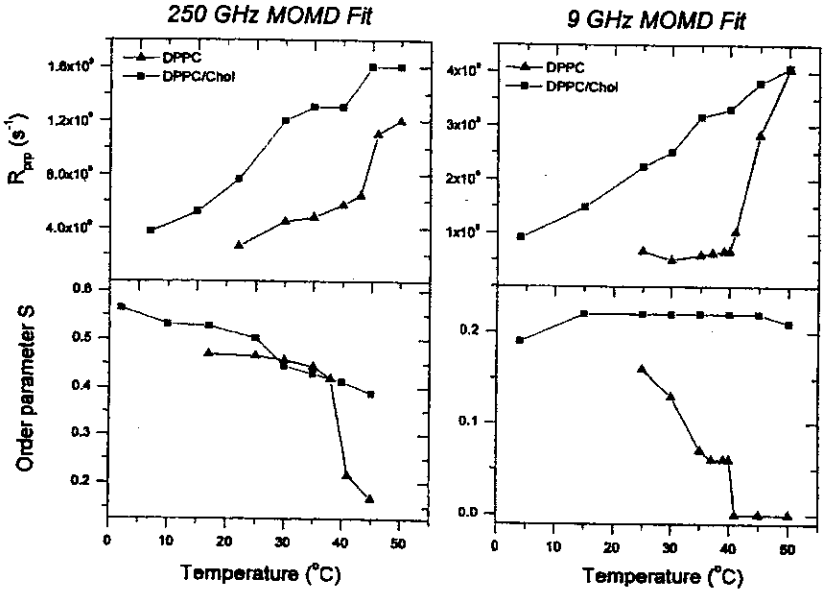

Figure 9. Rotational Diffusion rates and Order parameters of 16PC in membranes from 250 GHz and 9 GHz ESR spectra obtained their respective MOMD fits [11].

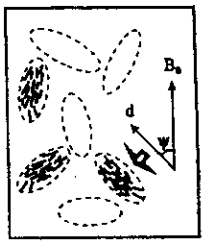

Figure 10. Dispersion sample for illustration of MOMD model.
B_0 magnetic field, **d** director axis and Ψ director tilt angle. All angles Ψ exist in the macroscopically disordered sample.

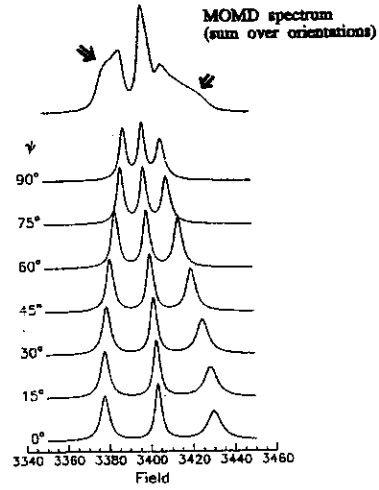

Figure 11. Absorption cw-ESR MOMD spectrum which is composed of the component spectra shown as a function of director tilt.

4. TWO DIMENSIONAL ELECTRON SPIN RESONANCE

4.1. Two-dimensional Fourier transform (FT) ESR and dynamic structure of membranes

Two-dimensional time domain ESR methods allow one to study both dynamics and

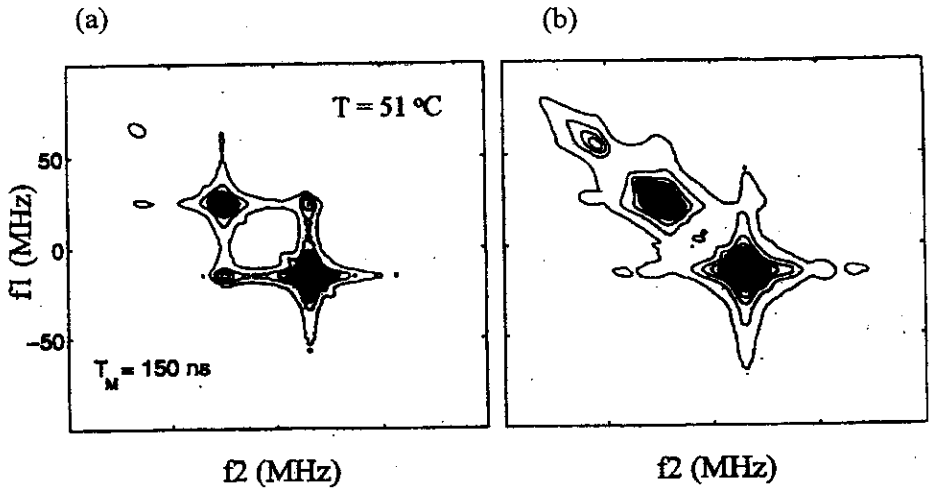

Figure 12. The 2D-ELDOR contours of (a) SM/16PC (Liquid crystal) and (b) SM/Chol/16PC (Liquid ordered) [10,12].

ordering in membrane vesicles [10,12,13]. In general, 2D ELDOR spectra from membrane vesicles exhibit more dramatic variations due to changes in membrane properties than do spectra obtained by cw ESR. Fig. 10 illustrates the challenge of a macroscopically disordered (i.e., MOMD) sample, such as from vesicles, micelles, micro-emulsions or LC polymers. We can define a local director axis **d** associated with the microscopic ordering.

Then Fig. 11 shows the absorption cw-EPR spectra as a function of director tilt. The observed spectrum based on MOMD is shown at the top and results from the summation over all orientations.

Fig. 12 shows the contours of the 2D ELDOR of 16PC observed in the LC and LO phases respectively in samples of (sphingomyelin) SM/16PC in the LC phase and SM/Chol/16PC in the LO phase [10,12], similar to those vesicle samples in the previous section. These sharply different spectra show that 2D-ESR dramatizes the differences in dynamic structure between liquid crystalline and liquid ordered phases. The results of

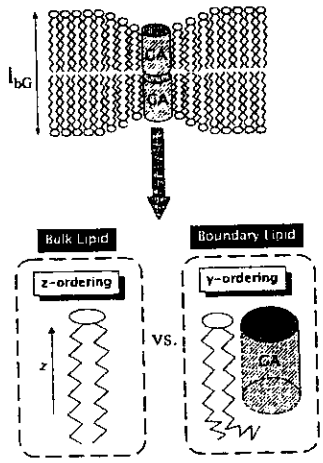

Figure 13. Two kinds of lipids; bulk and boundary lipids respectively suffer different z- and y-orderings.

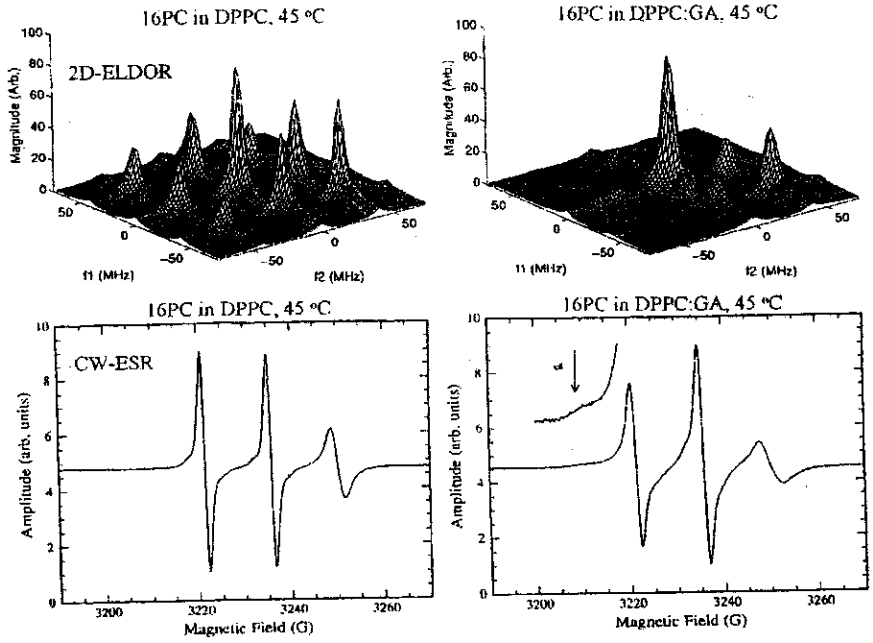

Figure 14. Comparison of cw and 2D FT ESR observed at 45C in pure and GA incorporated lipid vesicles [12].

this study may be summarized as follows:

(1) A MOMD analysis of 2D-ELDOR yields results closer to those from 250 GHz cw than 9 GHz cw ESR.

(2) 2D-ELDOR is more sensitive to the spin relaxation, which is dominated by the faster internal modes.

(3) Time Domain ESR differentiates between homogeneous and inhomogeneous broadening.

4.2. Lipid Protein interactions studied by two-dimensional ELDOR

The merits of 2D FT ESR spectroscopy are well demonstrated in studies of the effect of the peptide gramicidin A (GA) on the dynamic structure of model membranes. Besides bulk lipids, boundary lipids that coat the peptide are present but are difficult to resolve in cw ESR.

Fig. 13 illustrates the two kinds of lipids in the dynamic structure of membranes containing GA.

Fig. 14 shows a comparison of cw and 2D FT ESR observed at 45°C in pure and GA incorporated lipids [12]. Much more dramatic differences are observed in 2D FT ESR vesicles.

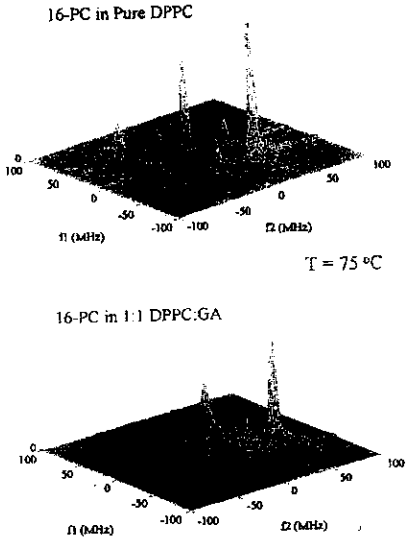

Figure 15. 2D FT ESR spectra (with short dead time) of 16PC showing boundary and bulk lipids in the presence of GA [10].

2D-FT ESR spectra obtained with very short dead times (25ns) show distinct signals from both boundary and bulk lipids [10, 12], cf. Fig.15. These experiments show that the boundary lipids experience a moderate decrease in motional rates but substantial orientational ordering changes.

ACKNOWLEDGEMENT

The author is grateful to the ShinSedai Research Institute for providing the travel funds to present this lecture at APES'01 and owes very much to Prof. Asako Kawamori, Chairperson of this symposium for the arrangement of this review. The work reported herein was supported by grants from NIH/NCRR, NIH/GM, and NSF, and was performed by many members of the Freed Research Group.

REFERENCES

1. L.J.Berliner, Ed., Spin Labeling: Theory and Applications (Academic Press, New York, (1976).
2. D.E. Budil, S. Lee, S. Saxena, J.H. Freed, J. Magn. Reson. A120 (1996) 155.
3. J.H. Freed, Annu. Rev. Biophys. Biomol. Struct. 23 (1994) 1.
4. G.R. Eaton, S.S.Eaton, L.J. Berliner, Eds., Distance Measurements in Biological Systems

by EPR, vol 19 of Biological Magnetic Resonance (Kluwer, NewYork 2000)
5. A.D. Milov, A.G. Maryasov, Yu. D. Tsvetkov, Appl. Magn. Reson. 15 (1998) 107
6a. P.P. Borbat, J.H. Freed, Chem. Phys. Lett. 313 (1999) 145; Ref. 4, Ch. 9 (2000).
6b. P.P. Borbat, H.S. Mchaourab, J.H. Freed, J. Am. Chem. Soc. (2002) submitted.
7. Z. Liang, J.H. Freed, J.Phys. Chem. B. 103 (1999) 6384
8. J.P. Barnes, Z. Liang, H.S. Mchaourab, J. H. Freed, and W.L. Hubbell Biophys. J. 76, (1999) 3298
9. Z. Liang, A.M. Bobst, R.S. Keyes. J.H. Freed, J.Phys. Chem. B. 104 (2000) 5372
10. P.P. Borbat, A.J. Costa-Filho, K.A. Earle, J.K. Moscicki, and J.H. Freed, Science, 291 (2001) 266
11. Y. Lou, M. Ge, J. H. Freed, J. Phys. Chem, 105 (2001) 11053
12. G. Patyal, R.H. Crepeau, J.H. Freed, Biophys. J. 73 (1997) 2201
13. J.H. Freed, Annu. Rev. Phys. Chem. 51 (2000) 655